Prediction of Free Surface Flows Relevant to PTS Problems

ALEXANDER CHURBANOV
Nuclear Safety Institute, Russian Academy of Sciences
52 B. Tul'skaya, Moscow 115191
RUSSIA
achur@ibrae.ac.ru http://www.ibrae.ac.ru

Abstract: This paper deals with assessment of two CFD codes (commercial code FLUENT and free/open source software OpenFOAM) for predicting free surface flows relevant to Nuclear Reactor Safety (NRS). Three validation cases attributed to Pressurized Thermal Shock (PTS) problems are calculated and compared with experimental data. The numerical results are in good agreement with measurements for all cases considered in the work. Both codes provide high-fidelity predictions of free surface flows and can be extensively exploited for reactor safety analysis.

Key-Words: Pressurized thermal shock, free surface flows, validation cases, FLUENT, OpenFOAM

1 Introduction

Nowadays is a strong trend does exist towards the use of Computational Fluid Dynamics (CFD) for solving problems of nuclear safety. Naturally, this results in the question what specific problems of practical importance we can study via CFD codes and how reliable are the results obtained numerically using computational tools.

The paper [1], which represents the results obtained by several teams working on the application of CFD codes to NRS issues, analyzes and systematizes particular problems of nuclear power industry, where the use of CFD brings positive results. One of these challenges is PTS problems, which occur during a number of accidents in reactors of various types and are characterized, among other phenomena, by free surface flows [2].

PTS in general denotes the occurrence of thermal loads on a reactor pressure vessel under the pressurized conditions. PTS was identified as one of the most important industrial needs related to NRS since the integrity of the reactor vessel has to be assured throughout the complete reactor life. A very severe PTS scenario is the cold water injection into the cold leg during accidents with a hypothetical small loss of coolant. The injected water mixes with a hot fluid presented in the cold leg and the derived mixture flows towards the downcomer, where further mixing with the ambient fluid takes place. Thus, thermal-hydraulic phenomena occurring in the cold leg at accidental cooling are characterized by various flow regions and many effects including their interaction. Namely, there are free liquid jets, zones of an impinging jet, regions of horizontal flows with free surface and so on.

The present work is concerned with numerical simulation of flows, which are typical for PTS problems with emphasis on free surface flows. Using commercial code FLUENT [3], predictions of jet flows have been conducted. Validation calculations have been performed for two tests from the ECORA project [4]. These are test VAL01 – an air jet impinging on a hot plate (a classical single-phase case from the ERCOFTAC Classic Collection Database [5], case C25) - and the VAL02 case – an impinging water jet in the air environment, which provides the first two-fluid flow considered here. Next, a cross-verification of FLUENT and free/open source software OpenFOAM [6] has been carried out using Test 2 from SPHERIC [7] (ERCOFTAC Special Interest Group for Smoothed Particle Hydrodynamics). In this test, which provides a variant of dam-breaking problems, a transient fluid flow with a wavy evolution of the free surface is considered in a tank. Both codes employed in our calculations are general purpose CFD codes and allow to model free surface flows using some implementations of the Volume-Of-Fluid (VOF) algorithm.

2 Air Jet Impingement with Heat Transfer

The first ECORA validation case VAL01 is an air jet impingement on a plate with heat transfer. This problem has no free surface. Here emphasis is on heat transfer in a single-phase air jet in air environment. The purpose of this test is to evaluate the accuracy of the convective heat transfer

predictions for turbulent jets. Jet impingement with heat transfer occurs in many PTS scenarios, where cold water is injected into the cold leg.

The VAL01 case considers an axisymmetric turbulent jet impinging orthogonally on a large plane surface, which is heated through the uniform heat flux q_w = 300 W/m^2. The flow is statistically steady-state and the fluid is air at the normal conditions. The flow in the pipe of diameter D = 0.026 m has the developed turbulent profile at the constant temperature T_0 = 20 °C. The Reynolds number of the problem $Re = U_b D\rho/\mu$ = 23, 000 is defined via the diameter of the pipe, the bulk velocity U_b = 12.922 m/s in the pipe, the density ρ and the dynamic viscosity μ. The height of the jet discharge above the plate is $H = 2D$. Temperature differences between the heated plate and the air jet in the domain of measurements are about 10 °C. Figure 1 presents the geometry and boundary conditions of this flow.

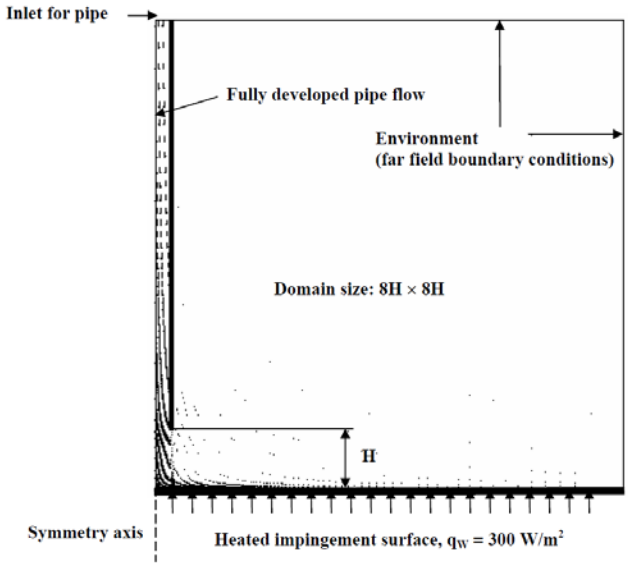

Fig. 1 Sketch of the VAL01 case

The impinging jet flow is the well-known validation case for evaluating turbulence models in the treatment of near wall regions. The stagnation region flow is dominated by normal straining of the fluid and so, many of widely-used models, which have been developed primarily for shear flow boundary layers, fail to predict the response of turbulence to normal straining.

Measured data for VAL01 were obtained in a lot of experiments and summarized in [5, case C25]. More resent experimental data are available, e.g., in [8-10]. The measurements include the mean velocity and stresses profiles along the vertical lines, which are parallel to the pipe axis and pass through the prescribed points on the plate surface. Next, there is available the radial distribution of the temperature T_w along the plate surface represented as the Nusselt number $Nu = q_w D/(T_w - T_0)/\lambda$, where λ is the air thermal conductivity. The numerical investigations [11-13] provide examples (among many others) of a comparative study, where the measurements are applied successfully for understanding merits and demerits of modern computational techniques for turbulence modelling in heat transfer problems. A similar analysis is presented below.

In the present calculations, which were performed using FLUENT, the problem was solved in the 3D formulation taking into account the symmetry of the flow. The computational domain has the height 4D and the radius 12D in order to avoid any influence of outflow boundary conditions. Buoyancy effects were omitted here, i.e., only forced convection was calculated due to small temperature differences and the large Reynolds number of the problem. Air was treated as an incompressible fluid with thermo-physical parameters corresponding to the normal conditions. No-slip, no-permeability conditions were imposed for the velocity on all rigid walls. Pipe walls were adiabatic whereas the uniform heat flux was given on the surface of the plate. On the remaining part of the boundary, which corresponds to the environmental conditions, the pressure outlet boundary conditions were specified.

The numerical scheme, which was employed for calculations by FLUENT, involved the following features:

- the SIMPLE scheme was used for steady-state calculations;
- the 2nd order QUICK approximations were employed for all equations. Some recommendations for selecting schemes to calculate convective heat transfer problems are available, e.g., in the recent study [14];
- the SST turbulence model was selected as the most reliable for heat transfer predictions [15].

To check the grid convergence of the numerical solution, calculations were performed on the following sequence of refining in space computational grids. Each successive grid was obtained from the previous one by decreasing the size of each cell by a factor of 1.5. The coarse grid #1 had 179 thousand cells, the medium grid #2 was about 513 thousand cells, and the fine grid #3 consisted of 1,245 thousand cells. Tetrahedral elements were used in the bulk of the computational domain, whereas stretching layers of prisms were employed near the solid walls for a good resolution of the hydrodynamic and thermal boundary layers.

The predicted velocity vector field on the symmetry plane of the computational domain (the stagnation zone only) is depicted in Fig. 2.

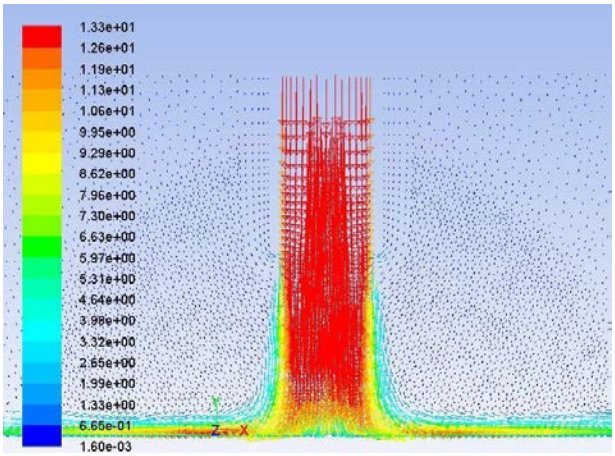

Fig. 2 The velocity vector field on the symmetry plane

In the experiments, there were measured profiles of the mean velocity along the lines in the domain of the maximal curvature of the streamlines near the impingement region. Figure 3 shows a comparison of the experimental normalized mean velocity profile from [5, case C25] with the predictions at the vertical line passing through the point r/D = 1. These numerical results were obtained on the fine grid #3, where the maximal y^+ value on the plate surface did not exceed 0.5. Obviously, a very good agreement between calculations on the fine grid and the measurements is observed. This is true for all other locations of measurements for the hydrodynamic parameters.

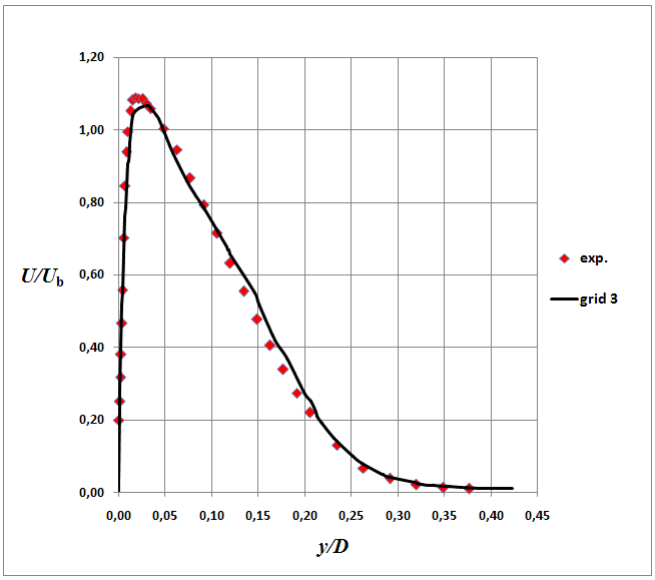

Fig. 3 Mean velocity profile along the vertical line through the point r/D = 1

As it was recommended in [4] for this problem, the main target variables are the maximum Nusselt number along the flat plate and the Nusselt number distribution as a function of the radius. A comparison of experimental radial distribution of the Nusselt number taken from [5, case C25] with the results of the present calculations on the sequence of grids is depicted in Fig. 4. Experiments indicate that the Nusselt number demonstrates essentially non-monotonic behaviour in the vicinity of the jet axis, and this peculiarity depends on the Reynolds number value. The numerical results obtained on the fine grid #3 demonstrates some discrepancies near the jet axis, where the distribution is non-monotonic, but, in general, are close enough to the measurements.

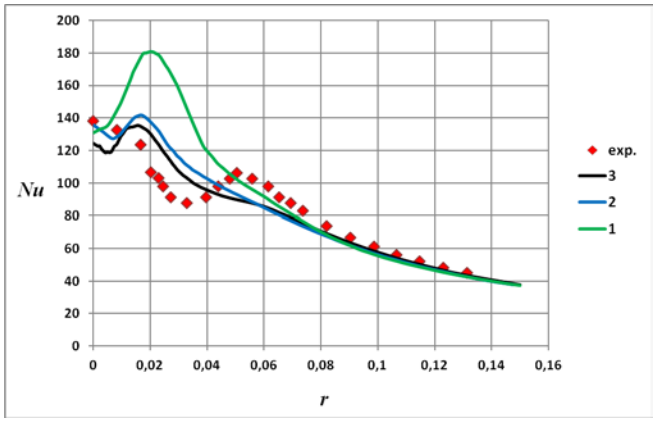

Fig. 4 Radial distribution of the Nusselt number

In general, with the correct choice of a turbulence model, FLUENT provides a good agreement of numerical results with experiments for jet flows with heat transfer. Some discrepancies are explained by general limitations of the eddy viscosity models, which are employed in CFD codes.

3 Water Jet in Air Environment

A water jet in air environment impinging on an inclined flat plate is studied in test VAL02. It is the turbulent two-phase flow involving two immiscible fluids with free surface that represents cold water injection in the steam filled cold leg. Figure 5 demonstrates the geometry of this test as well as the computational domain. The complete description of this problem is available in the experimental-numerical work [16] or predictions [17].

The axisymmetric jet of water flows from the pipe into the air and impinges on the solid plate inclined with the angle 30º to the pipe axis. The geometrical parameters of the pipe part involved in

calculations are s = 0.01 m and h = 0.08 m, the axis distance between the pipe outlet and the plate is H = 0.1 m, the pipe diameter D = 0.03 m, and the circular part of the plate that is included into the computational domain has the diameter 20D.

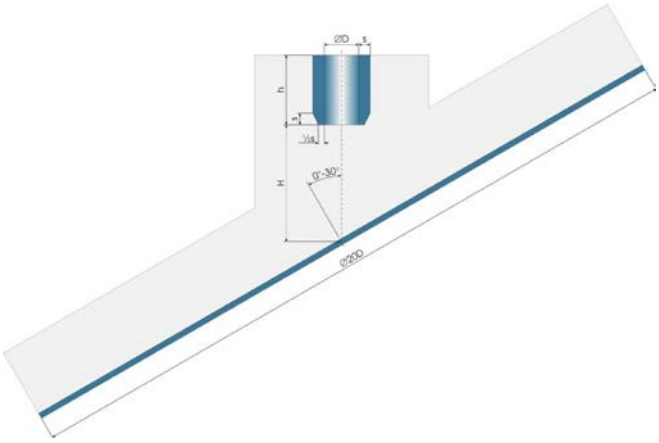

Fig. 5 Sketch of case VAL02

The flow under the consideration is steady-state at the normal conditions. The bulk water velocity in the pipe is U_b = 19.8 m/s, which gives the Reynolds number of the problem $Re = U_b D\rho/\mu = 5.9\times10^5$ corresponding to the turbulent flow regime. Here ρ is the density and μ stands for the dynamic viscosity. In the experiments [16], the pressure p on the plate surface was measured and represented as the dimensionless pressure coefficient $C_p = (p-p_0)/(1/2\rho U_b^2)$.

This free surface problem was solved in the 3D formulation with the symmetry plane taking into account the gravity effects. Water and air were considered as incompressible fluids. On the pipe inlet, there was specified the normal velocity component with the parameters of turbulence corresponding to the weak level of turbulence in the flow: the turbulence intensity was Tu = 1% only, the ratio of the eddy viscosity to the molecular viscosity was equal to 10. On the remaining part of the boundary, which corresponds to the environmental conditions, the pressure outlet boundary conditions were specified.

To obtain the steady-state solution, any suitable initial water-air distribution can be chosen. In the initial conditions applied here, only the pipe was occupied by the water. The jet formation with the following spreading of water over the plate was tracked in the time-dependent calculations.

The calculations via FLUENT have been conducted using the homogeneous multi-phase flow model (see [18] for a detailed description and recommendations for practical use) with the following options of the numerical algorithm:

- time-dependent equations were approximated using the PISO operator-splitting scheme. The steady-state solution was derived as the limit of the time-evolution process;
- the convective terms in all equations were approximated by the QUICK scheme;
- the SST model was included to take into account the turbulence effects;
- the explicit variant of the VOF method in the iteration-free formulation NITA was employed to describe the evolution of the water-air interface with a variable time-step satisfying the Courant number restriction of 0.25.

This selection of numerical parameters is based on recommendations from the FLUENT documentation.

As in the previous case, the sequence of three spatial grids was used to check the grid convergence of the numerical solution. Each successive grid was obtained from the previous one by decreasing the size of each cell by a factor of 1.5. The latest versions of FLUENT make possible to perform a conversion of tetrahedral cells into polyhedral ones. The aim of this operation is to reduce essentially (approximately by a factor equals 4) the number of grid cells. In addition, the use of such polyhedral grids results in a higher convergence rate of the numerical solution.

In our calculations with FLUENT on the basis of polyhedral grids, the coarse grid #1 was small enough (104 thousand cells), the medium grid #2 was about 218 thousand cells, and the fine grid #3 has more than 503 thousand cells. Polyhedral elements were used in the domain occupied by the air. In the water jet domain, hexahedral cells were employed that provided a more accurate tracking of the water-air interface. Stretching layers of prisms were applied near the solid walls of the pipe and plate for a better resolution of the boundary layer. The maximal y^+ value on the plate surface for the fine grid was 0.8.

The steady-state solution obtained on the fine grid is shown below. Figure 6 demonstrates the steady-state velocity vector field on the symmetry plane of the computational domain.

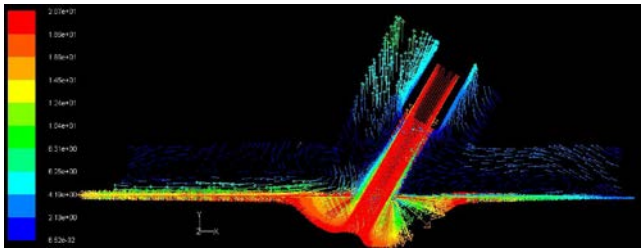

Fig. 6 The velocity vector field on the symmetry plane

The distribution of the water volume fraction f is depicted in Fig. 7 on the symmetry plane. The red colour (f = 1) corresponds to the water, whereas the blue colour (f = 0) shows the air. Intermediate values/colours indicate some smearing of the water-air interface due to the VOF algorithm features and visualization effects. This smearing of the interface includes 2-3 grid cells that is a good property for the implementation of the VOF method in FLUENT.

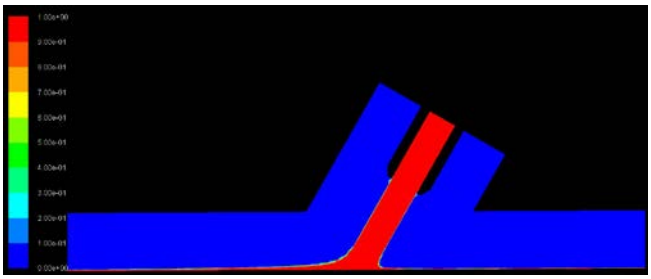

Fig. 7 Steady-state distribution of water volume fraction on the symmetry plane

A comparison of the experimental data from [16] with our calculations on all three computational grids is shown in Fig. 8. The pressure coefficient C_p is presented along the plate surface on the symmetry plane versus the dimensionless coordinate x/D, which has zero value at the point of intersection of the pipe axis with the plate surface. For all three grids, we observe a good agreement of numerical results with measurements.

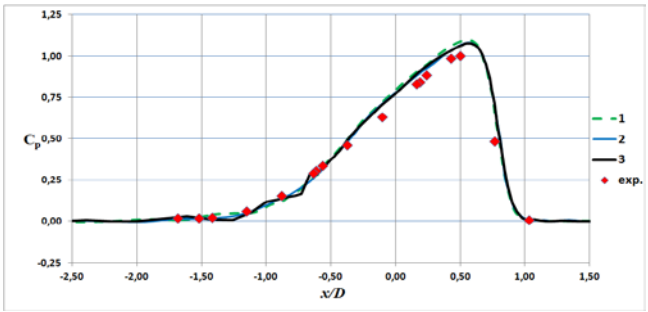

Fig. 8 Distribution of C_p along the plate surface on the symmetry plane

The above comparisons show that code FLUENT with the applied free surface flow model and turbulence model provides accurate predictions of jet flows with free surfaces.

4 Dam-Breaking Flow over an Obstacle

A transient 3D dam-breaking flow in a tank with a small obstacle is calculated in this case. This is a simplified example of stratified two-phase flows occurring in PTS problems. All measurements are available from the site of ERCOFTAC SPHERIC special interest group [7,19].

Figure 9 shows the geometry of the problem as well as the lines and points of measurements. In a rectangular tank filled with air and having at the flat bottom a small solid rectangular box, a part of the volume is occupied by water separated from air by the partition (it is not shown in the figure) and having the initial form of the blue box. After instantaneous removal of the partition, water under the influence of gravity spreads over the tank making oscillating movements between its the left and right walls up to reaching the state of complete rest. This figure presents all geometrical parameters of the problem as well as the points of measuring the pressure (points P1-P8 on the front and top surfaces of the box) and lines of measuring the vertical height of water (probes H1-H4). Moreover, instantaneous flow patterns are available from experiments at some time moments.

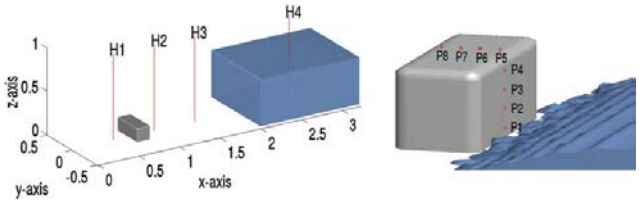

Fig. 9 Sketch of the dam-breaking flow with the lines and points of measurements

The 3D formulation with the symmetry plane was used in the present computations. Water and air were treated as incompressible immiscible fluids with physical parameters corresponding to the normal conditions. The problem was solved in the laminar formulation omitting the wettability and surface tension, which are negligible under the conditions considered. As for the initial configuration for simulations, the water in the dam domain was at rest.

The calculations with FLUENT have been conducted with the following options:

- The PISO scheme was used for time-stepping;
- The convective terms in all equations were approximated by the QUICK scheme;
- The explicit variant of the VOF method in the iterative formulation ITA was used to describe the evolution of the water/air interface with a fixed time step τ;
- The geometric reconstruction method based on a piecewise linear representation of the interface between the phases was employed.

This selection of numerical parameters is based on recommendations from the FLUENT

documentation and numerical investigations of this problem [20-23].

Only two computational grids were used due to high computational costs of such transient PC-based calculations. Namely, the coarse grid #1 had 115 thousand cells, whereas the medium grid #2 used 366 thousand cells, respectively. Grid #2 was obtained from the grid #1 via reduction of each cell by a factor of 1.5 in size. Hexahedral cells were used in both grids with stretching outwards the bottom.

To check the independence of the numerical results from a time-integration step, the set of calculations was performed with three different time step $\tau = 0.002$, 0.001, and 0.0005 s, respectively. All calculations were carried out up to time moment of 6 seconds, when practically the full rest state was observed in the experiments.

A comparison of the results obtained at various spatial and temporal grids have showed that for this problem it is sufficient to use the time step $\tau = 0.001$ s with the medium spatial grid #2; this provides the results practically unimproved in sense of accuracy. The results derived on this spatial-temporal grid are presented below.

A comparison of calculations via FLUENT with experiments is presented in Figures 10 and 11 for the time-dependent data at two locations. These two figures show the time-histories for the height of the water layer defined at the probes H4 and H2, respectively. The line H4 passes practically through the midpoint of the initial water dam/box, whereas the line H2 is located in front of the rectangular solid box. The position of the water-air interface in the calculations is evaluated by the value of the water volume fraction $f = 0.5$. For the probe H4, a very good agreement of the numerical results with experimental data is observed in Fig. 10.

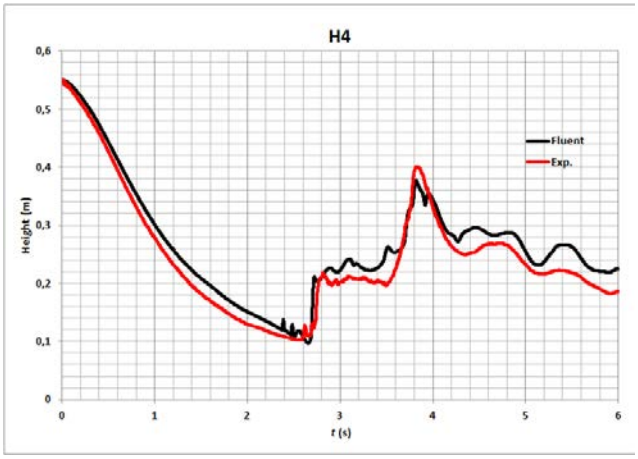

Fig. 10 Time-history of the water height at probe H4

For the line H2, in the time interval between 1.5 and 2.5 s, our calculations indicate some oscillations, which are absent in the experiments. It can be observed clearly in Fig. 11. The remaining sections of the calculated and experimental curves are rather close to each other. This time interval corresponds to the maximum deformation of the free surface in the left half of the tank, and possibly, it can be predicted more accurately by using a refined computational grid in space.

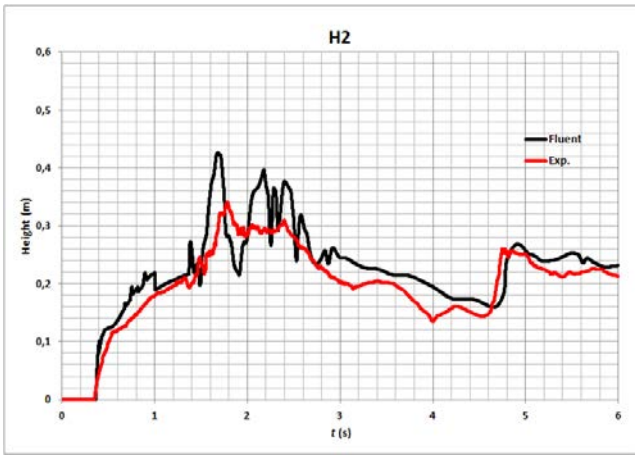

Fig. 11 Time-history of the water height at probe H2

Further figures demonstrate a cross-verification of two CFD code, i.e., FLUENT versus OpenFOAM.

Similar calculations of this test have been conducted using code OpenFOAM on the same spatial grid #2. To describe the evolution of the water-air interface, there was used the MULES variant of the VOF method with fixed time step $\tau = 0.001$ s. All parameters of the numerical scheme were selected similarly to the FLUENT scheme (where it was possible).

Figure 12 shows the instant water volume fraction field on the symmetry plane at the time moment $t = 0.4$ s, when in the experiment the water layer for the first time reaches the obstacle. The upper pattern demonstrates the results predicted by FLUENT; the lower numerical snapshot corresponds to the computations carried out via OpenFOAM.

Here the red colour refers to the water, whereas the blue one indicates the air. Obviously, both codes give very close numerical results, which are smooth enough at this initial stage of the water spreading. Moreover, they are in a good agreement with the experimental instantaneous flow pattern [7,19] (experiment data are not shown in this figure).

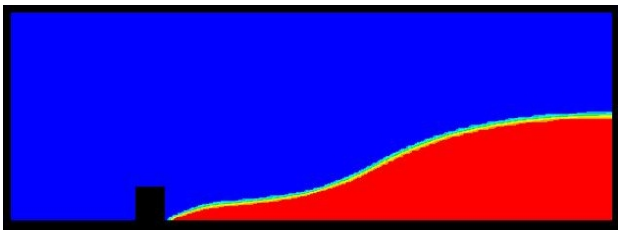

(a) FLUENT

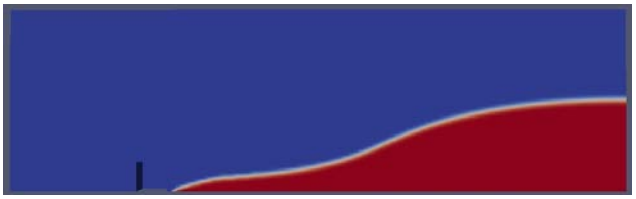

(b) OpenFOAM

Fig. 12 Water volume fraction field at t = 0.4 s. Predictions via (a) FLUENT; (b) OpenFOAM

This cross-verification of two CFD codes is continued below.

Figure 13 presents the water-air interface on the symmetry plane at the time moment t = 0.56 s.

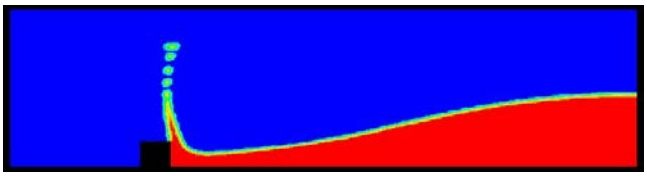

(a) FLUENT

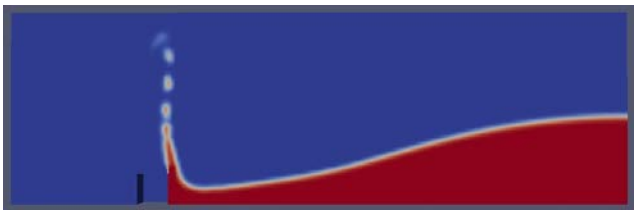

(b) OpenFOAM

Fig. 13 Water volume fraction field at t = 0.56 s. Predictions via (a) FLUENT; (b) OpenFOAM

This moment corresponds to the strong deformation of the free surface above the rigid obstacle with formation of the water plume and drops observed in the experiments. The experimental free surface for the time moment t = 0.56 s is depicted in Fig. 14 reproduced from measurements [7,19]. The flow pattern is shown in two parts – inside (the small top-right figure) and outside (the general figure) of the dam.

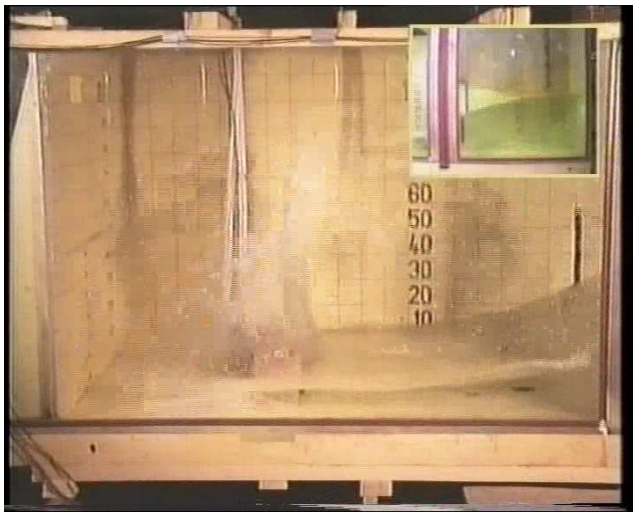

Fig. 14 The experimental free surface pattern at t = 0.56 s

The corresponding 3D water-air interface obtained by FLUENT for t = 0.56 s is presented in Fig. 15 in the whole computational domain.

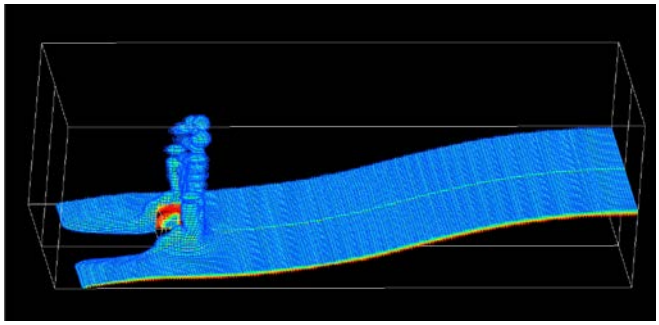

Fig. 15 The water-air interface at t = 0.56 s predicted by FLUENT

In this figure, we see a good qualitative agreement between the numerical results and the above experimental pattern.

Despite of some differences in the numerical algorithms implemented in FLUENT and OpenFOAM in order to track moving free surfaces, we observe here a very good agreement of the numerical results with each other and with the experimental data.

A more quantitative comparison of calculations via codes FLUENT and OpenFOAM is presented in Figures 16 and 17. They show the calculated time-histories of the pressure at points P1 and P5 located at the front side and the top of the obstacle, respectively. In addition, the measurements are also plotted in these figures.

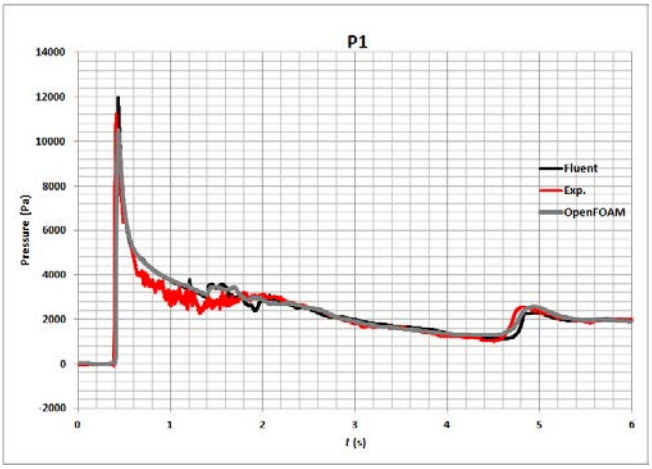

Fig. 16 Time-history of the pressure at point P1

It is easy to see from Fig. 16 that the numerical results at the point P1 obtained using these two CFD codes are almost identical and agree very well with measurements.

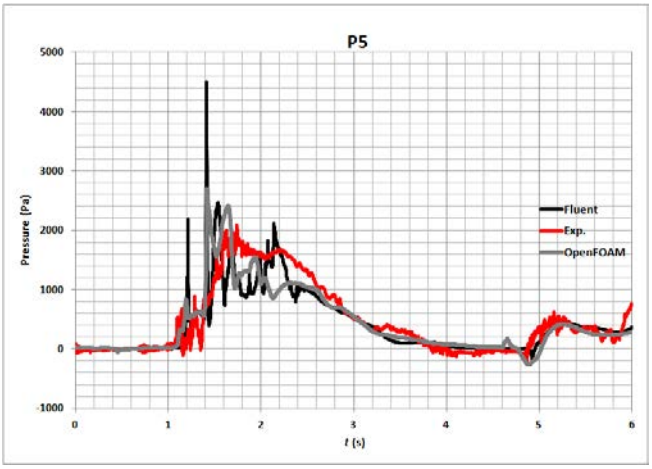

Fig. 17 Time-history of the pressure at point P5

As for the pressure at the point P5, calculations in the time interval between 1.5 and 2.5 s demonstrate some oscillations, which are absent in the experiment (see Fig. 17). In this case, OpenFOAM gives smaller deviations from the experiments in compare with code FLUENT. It should be noted that similar wiggles in the pressure were obtained in the calculations of other authors [20-23] who used their own in-house codes. The remaining parts of the calculated and experimental curves are rather close to each other. As mentioned above, this time interval corresponds to the maximum deformation of the free surface resulting from an impact of water on the left wall of the cavity. For a more accurate description of this flow, it is necessary to use a refined spatial grid in the vicinity of the rectangular box.

Therefore, both CFD codes - FLUENT and OpenFOAM - demonstrate very similar results in the calculation of the MARIN dam-breaking test. Despite of some discrepancies within the time interval between 1.5 and 2.5 s, the coincidence of the calculations with the experimental data can be considered as very satisfactory.

5 Summary and Conclusions

An analysis of capabilities of two up-to-date CFD codes to predict free surface flows relevant to NRS is performed in the present study.

Three validation cases arising in the PTS problems have been simulated using the commercial CFD code FLUENT. Two turbulent jets - with and without heat transfer as well as with and without free surface - were predicted using FLUENT. In addition, a cross-verification of FLUENT with free/open source software OpenFOAM was performed on the dam-breaking flow.

The results obtained indicate that both codes demonstrate a good accuracy of predictions for free surface flows. The PC-based calculations conducted in the work are in good agreement with measurements for all cases under the consideration.

Predictions of free surface flows with FLUENT demonstrate appropriate accuracy. Performed calculations are in good agreement with measurements for all considered cases. OpenFOAM provides a good enough agreement both with experimental data and predictions via FLUENT. Both codes provide high-confidence predictions of free surface flows and can be extensively exploited for reactor safety analysis. This fact explains clearly a new trend in CFD that appears recently for solving industrial problems, i.e., to refuse from using commercial general-purpose software in favor of free/open source software. This allows to construct easy-to-use mathematical tools oriented to solving specific user-oriented problems with its possible tuning and improvement in the future.

References:

[1] Assessment of Computational Fluid Dynamics (CFD) for Nuclear Reactor Safety problems, NEA/CSNI/R (2007)13, 2008.

[2] Y. Bartosiewicz, J.-M. Seynhaeve, C. Vallee *et al.*, Modeling Free Surface Flows Relevant to a PTS Scenario: Comparison Between Experimental Data and Three RANS Based CFD-Codes. Comments on the CFD-Experiment Integration and Best Practice

Guideline, *Nucl. Eng. Des.*, Vol.240, 2010, pp.2375-2381.

[3] FLUENT 6.3 User's Guide, Fluent Inc., 2006.

[4] M. Scheuerer, M. Heitsch, F. Menter *et al*., Evaluation of Computational Fluid Dynamic Methods for Reactor Safety Analysis (ECORA), *Nucl. Eng. Des.*, Vol.235, 2005, pp.359-368.

[5] http://cfd.mace.manchester.ac.uk/ercoftac/index.html

[6] OpenFOAM: The Open Source CFD Toolbox. User Guide v.1.7.0, OpenCFD Ltd., 2010.

[7] http://www.ercoftac.org/special_interest_groups/40_smooth_particle_hydrodynamics/ (https://wiki.manchester.ac.uk/spheric/index.php/Main_Page)

[8] N. Zuckerman and N. Lior, Jet Impingement Heat Transfer: Physics, Correlations, and Numerical Modeling, In: *Advances in Heat Transfer*, Vol.39, Elsevier, Amsterdam, 2006, pp.565-631.

[9] V. Katti and S.V. Prabhu, Experimental Study and Theoretical Analysis of Local Heat Transfer Distribution Between Smooth Flat Surface and Impinging Air Jet from a Circular Straight Pipe Nozzle, *Int. J. Heat Mass Transfer*, Vol.51, 2008, pp.4480-4495.

[10] M.J. Tummers, J. Jacobse and S.G.J. Voorbrood, Turbulent Flow in the Near Field of a Round Impinging Jet, *Int. J. Heat Mass Transfer*, Vol.54, 2011, pp.4939-4948.

[11] S.O. Neumann, N. Uddin and B. Weigand, Grid Sensitivity of LES Heat Transfer Results of a Turbulent Round Impinging Jet, In: W.E. Nagel *et al.* (eds.), *High Performance Computing in Science and Engineering'10*, Springer-Verlag, Berlin, 2011, pp.307-325.

[12] L. Del Frate, M.C. Galassi, F. D'Auria *et al*., CFD Simulations of a Normally-Impinging Jet from a Circular Nozzle, *Proc. 20th Int. Conf. "Nuclear Energy for New Europe 2011"*, Bovec, Slovenia, Sept. 12-15, 2011, pp.820.1-820.10.

[13] S. Kubacki and E. Dick, Hybrid RANS/LES of Flow and Heat Transfer in Round Impinging Jets, *Int. J. Heat Fluid Flow*, Vol.32, 2011, pp.631-651.

[14] M. Goodarzi, M.R. Safaei, A. Karimipour *et al.*, Comparison of the Finite Volume and Lattice Boltzmann Methods for Solving Natural Convection Heat Transfer Problems inside Cavities and Enclosures, *Abstract and Applied Analysis*, Vol.2014, Article ID 762184, 15 pages, 2014.

[15] F.R. Menter, M. Kuntz and R. Langtry, Ten Years of Industrial Experience with the SST turbulence Model, In: K. Hanjalic *et al.* (eds.), *Turbulence, Heat and Mass Transfer 4*, Begell House, 2003, pp.625-632.

[16] S. Kvicinsky, Methode d'Analyse des Ecoulements 3D a Surface Libre: Application aux Turbines Pelto, PhD Thesis, EPFL, Lausanne, 2002.

[17] B. Zoppe, C. Pellone, T. Maitre *et al*., Flow Analysis Inside a Pelton Turbine Bucket, *ASME J. Turbomachinery*, Vol.128, 2006, pp.500-511.

[18] G. Tryggvason, R. Scardovelli and S. Zaleski, *Direct Numerical Simulations of Gas-Liquid Multiphase Flows*, Cambridge University Press, Cambridge, UK, 2011.

[19] R. Issa and D. Violeau, 3D dambreaking, ERCOFTAC SPHERIC SIG Test-case 2, 2006 (https://wiki.manchester.ac.uk/spheric/index.php/Main_Page).

[20] I.R. Park, K.S. Kim, J. Kim *et al*., A Volume-of-Fluid Method for Incompressible Free Surface Flows, *Int. J. Numer. Methods Fluids*, Vol.61, 2009, pp.1331-1362.

[21] E.F. Lins, R.N. Ellas, F.A. Rochinha *et al*., Residual-Based Variational Multiscale Simulation of Free Surface Flows, *Comput. Mech.*, Vol.46, 2010, pp.545-557.

[22] A. Di Monaco, S. Manenti, M. Gallati *et al*., SPH Modeling of Solid Boundaries through a Semi-Analytic Approach, *Eng. Appl. Comput. Fluid Mech.*, Vol.5, 2011, pp.1-15.

[23] P. Ortiz, Non-Oscillatory Continuous FEM for Transport and Shallow Water Flows, *Comput. Methods Appl. Mech. Engrg.*, Vol.223-224, 2012, pp.55-69.